Heterogeneous Catalysis

DOI: 10.1002/anie.200702534

High-Activity, Single-Site Mesoporous Pd/Al_2O_3 Catalysts for Selective Aerobic Oxidation of Allylic Alcohols**

*Simon F. J. Hackett, Rik M. Brydson, Mhairi H. Gass, Ian Harvey, Andrew D. Newman, Karen Wilson, and Adam F. Lee**

The heterogeneously catalyzed aerobic selective oxidation of hydrocarbons offers new, environmentally benign routes to a diverse range of valuable intermediates for the pharmaceutical, fine chemical, and agrochemical sectors.[1] Such powerful catalytic technologies circumvent the use of stoichiometric reagents and expensive homogeneous complexes along with the associated process disadvantages and safety issues.[2] While there has been recent interest in the potential of gold as a partial oxidation catalyst,[3] such systems typically offer low oxygenate yields and require either radical initiators,[4] high temperatures, or high O_2 partial pressures.[5] Supported ruthenium,[6] palladium, and platinum clusters are also promising candidates to catalyze the selective oxidation (selox) of primary alcohols to their corresponding aldehydes under mild conditions.[7] These reactions are highly regioselective in the presence of diverse functionalities, including allylic groups. Most studies in this area employing Pd and Pt have utilized commercial formulations based upon amorphous carbon or oxide supports. However, the poor intrinsic performance of these materials relative to their homogeneous counterparts has often necessitated ad hoc promotion of the reaction by non-noble metals to achieve even moderate yields.[8] Two factors presently constrain the wider adoption of heterogeneous Pd selox catalysts amongst both academic and industrial communities: first, uncertainty over the active site responsible for the rate-limiting oxidative dehydrogenation step,[9] and second, the use of conventional supports with restrictive pore dimensions that inhibit efficient mass and heat transfer to and from reaction sites and limit the range of viable solvents and substrates.[10]

Recent studies have implicated surface palladium oxide as the active center in allylic alcohol selox.[11] Since the energetics of metal clusters increasingly favor oxide-terminated surfaces with decreasing cluster size,[12] we hypothesized that a mesoporous high-area support would serve to both stabilize highly dispersed palladium oxide nanoparticles and would facilitate efficient alcohol and aldehyde diffusion. Herein, we report the successful synthesis of tailored $Pd–Al_2O_3$ catalysts and demonstrate that extremely low palladium loadings generate atomically dispersed Pd^{II} surface species that confer exceptional selox activity of allylic alcohols.

Mesoporous alumina-supported palladium catalysts (Pd/meso-Al_2O_3) were prepared by a modified surfactant-templated route through hydrolysis of aluminum *sec*-butoxide and subsequent aging in the presence of lauric acid.[13] The organic template was removed by calcination prior to incipient wetness impregnation with tetraammine palladium(II) nitrate solution (see the Supporting Information). Samples were then calcined, reduced, and stored in air. Porosimetry and powder X-ray diffraction confirmed that the final processed materials possessed well-defined, hexagonal pore structures, with surface areas of 350 $m^2 g^{-1}$ and uniform 3-nm-diameter thick-walled pores. X-ray analysis provides clear evidence that the mesoporous support stabilizes palladium nanoparticles that are smaller than can be achieved using conventional amorphous aluminas. Furthermore, shrinking palladium nanoparticle dimensions from 4.5-nm to below 1.7-nm diameter induces a striking transition from surface-bound Pd^0 aggregates to isolated Pd^{II} sites. Palladium K-edge EXAFS analysis (Figure 1, EXAFS = extended X-ray absorption fine structure) reveals a strong signal from a Pd–Pd coordination shell at 2.75 Å for **B** (4.7 wt % Pd), indicative of large metallic Pd clusters. In sharp contrast, the ultradilute sample **C** (containing only 0.03 wt % Pd) possesses only four-coordinate Pd–O scatterers at 2.00 Å, akin to a truncated PdO environment.

Linear combination fitting of the corresponding X-ray absorption near-edge structure (XANES) data with oxide and metal standards verifies that mesoporous alumina stabilizes palladium in the +2 oxidation state. A weak shoulder in the edge threshold of **C** further indicates that palladium adopts a four-coordinate, pseudo-square-planar geometry similar to that in PdO;[14] this shoulder is absent for isotropic symmetries at Pd^{III} and Pd^{IV} centers.[15] X-ray photoelectron spectroscopy (XPS) corroborates this gradual evolution from metallic to oxidic surface palladium with decreasing cluster size (i.e. Pd loading).

The core-level chemical shift and near-edge absorbance of the atomically dispersed Pd^{II} species are indistinguishable from those of Pd^{II} residing within extended palladium oxide phases, despite their different coordination spheres. However,

[*] S. F. J. Hackett, A. D. Newman, Dr. K. Wilson, Dr. A. F. Lee
Department of Chemistry
University of York, York YO10 5DD (UK)
Fax: (+44) 1904-432-516
E-mail: afl2@york.ac.uk
Homepage: http://www-users.york.ac.uk/%7Eafl2/index.htm
Dr. M. H. Gass, Dr. I. Harvey
Daresbury Laboratory
Daresbury, Cheshire WA4 4AD (UK)
Prof. R. M. Brydson
Institute for Materials Research
University of Leeds, Leeds LS2 9JT (UK)

[**] We thank the EPSRC (EP/E046754/1, EP/P500575/1) and CCLRC (beamtime award 46106) for financial support of this work.

Supporting information for this article is available on the WWW under http://www.angewandte.org or from the author.

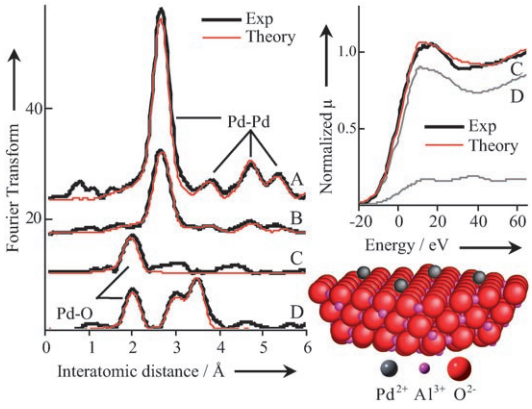

Figure 1. Left: Pd EXAFS of Pd foil (**A**), 4.7 wt% Pd/meso-Al_2O_3 (**B**), 0.03 wt% Pd/meso-Al_2O_3 (**C**), and PdO (**D**). Right: Fitted Pd XANES (theory corresponds to 15% **A** and 85% **D**) and schematic depiction of Pd bound in fourfold hollow sites on a (100)-terminated γ-alumina surface.

using high-resolution high-angle annular dark-field (HAADF) scanning transmission electron microscopy (STEM), it was possible to directly image these isolated Pd centers. Figure 2 shows a smoothed HAADF STEM image of the 0.03 wt% Pd/meso-Al_2O_3 sample; two pores of approximately 2.5 nm are apparent in the support in the center of the image. HAADF imaging is particularly sensitive to atomic number, with heavy atoms appearing brighter.[16] A large number of such bright spots are distributed across the alumina framework, with common diameters of approximately 0.13 nm, consistent with individual heavy atoms either on or within the support.[17]

Time-lapse imaging reveals that these bright spots are mobile, indicating movement across the pore walls of the support as a result of excitation from the focused electron beam and thus confirming the atomic nature of the spots. No larger aggregates were observed, although larger particles were seen at higher Pd loadings. Representative particle-size distributions are presented in the Supporting Information. It is impossible to identify such small particles or single atoms in low-Pd-loaded samples using standard TEM or in aberration-corrected bright-field imaging (see the Supporting Information for comparison).

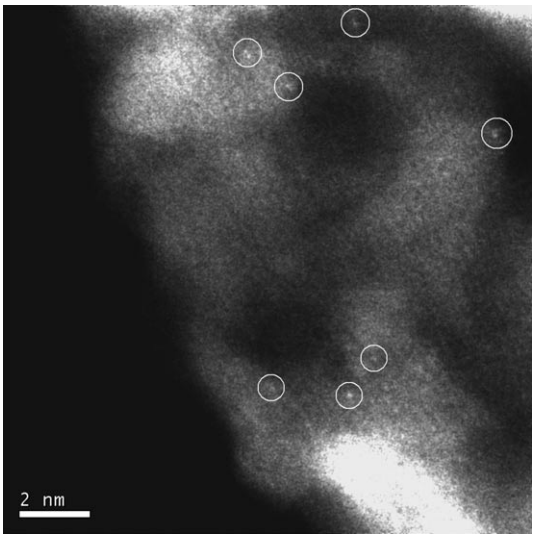

Figure 2. HAADF STEM image of a 0.03 wt% Pd/meso-Al_2O_3 sample.

The catalytic performance of mesoporous alumina-supported palladium clusters was subsequently explored in the aerobic selox of cinnamyl and crotyl alcohols to their corresponding aldehydes. Figure 3 shows the resultant turnover frequencies (TOF) per exposed surface Pd site for crotyl alcohol as a function of cluster size (loading) and total (oxide and single-site) Pd^{II} content. Metal dispersions were measured by H_2 chemisorption, while the total Pd^{II} concentration was derived from the fitted XANES spectra. The latter was in excellent agreement with the corresponding surface Pd^{II} concentration from XPS (Table 1), thus indicating that electron-deficient palladium was always surface-segregated (either as a capping surface PdO_x layer around metal cores, as small oxide particles, or as single sites, depending on the loading).

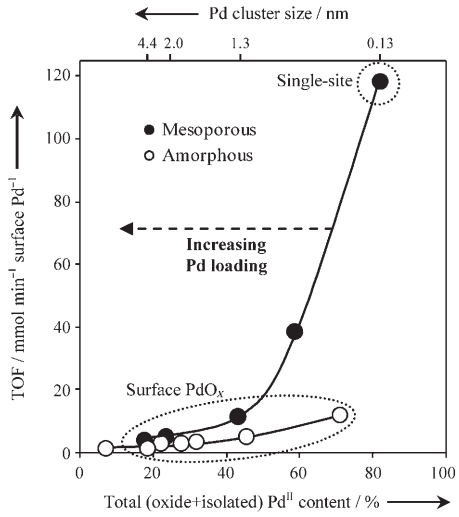

Figure 3. Catalytic performance of Pd clusters dispersed across conventional versus mesoporous alumina supports as a function of size and oxidation state in aerobic crotyl alcohol selox.

The impact of using a high-area, mesoporous alumina support compared with conventional γ-Al_2O_3 is dramatic. As the Pd loading and cluster size fall, the ability of the mesoporous support to stabilize atomically dispersed Pd^{II} sites confers a tenfold rate enhancement over the conventional system. The higher support surface area undoubtedly boosts palladium dispersion, resulting in clusters for similar loadings that are smaller than those achieved over the amorphous alumina (see the Supporting Information). However, another key factor may be a higher defect density within the transitional alumina phase formed in our mesoporous support.[13] Such defects are likely nucleation centers for palladium, and indeed, alumina surfaces have been recently shown to inhibit adatom diffusion and sintering of small Au particles.[18]

Table 1: Structural and catalytic properties of Pd/meso-Al_2O_3.

Catalyst [wt%]	Particle size[a] [nm]	Total Pd^{II} [%][b]	Surface Pd^{II} [%][c]	TON[d]	Yield [mmol h^{-1} $g_{cat.}^{-1}$][e]	Selectivity [%][f]
0.03	0.13	85	76.6	1305 (822)	3.1 (1.9)	91 (92)
0.06	0.8	59	57.2	1908 (678)	5.1 (1.8)	88 (92)
1.03	1.3	43.4	44.1	163 (50)	29.9 (9.0)	91 (91)
2.37	2.0	23.6	22.2	55 (18)	24.8 (8.2)	93 (90)
4.70	4.4	17.8	10.2	36 (16)	17.1 (7.2)	94 (89)

[a] Average from EXAFS 1st shell CN, X-ray line-broadening, and TEM. [b] From fitted XANES Pd K-edge spectra. [c] From fitted Pd 3d XP spectra. [d] Turnover number based on crotyl alcohol turnover per mole Pd after 1 h; cinnamyl alcohol values are given in parentheses. [e] Cinnamyl alcohol values are given in parentheses. [f] Selectivity for aldehyde; cinnamyl alcohol values are given in parentheses.

It is interesting to note the nonlinear dependence of TOF on the total Pd^{II} concentration, which reflects the structural evolution of supported palladium. We have previously shown that metallic Pd (dominant at high loadings) exhibits poor activity towards allylic alcohol selox.[11b] The slow initial rise in TOF in Figure 3 over both alumina supports is associated with the transition from large metal to small oxidic clusters that expose moderately active surface PdO_x. To confirm that the dramatic rate enhancement in the ultradilute regime for the Pd/meso-Al_2O_3 catalyst is attributable to the genesis of isolated Pd^{II} centers, apparent activation energies were measured for different loadings. These measurements indeed reveal two distinct regimes associated with the switch-over at approximately 0.06 wt% palladium as given in Equation (1):

$$\text{surface } Pd^{II}O_x \text{ phase} \rightarrow \text{atomically dispersed } Pd^{II} \text{ species}$$
$$\Delta E_{act} \approx 45 \pm 5 \text{ kJ mol}^{-1} \quad \Delta E_{act} \approx 10 \pm 5 \text{ kJ mol}^{-1} \qquad (1)$$

With TOF = 4400 h^{-1}, our 0.03 wt% Pd/meso-Al_2O_3 catalyst is the most active ever reported for heterogeneous cinnamyl alcohol oxidation. This result compares favorably with the best literature values of 538 h^{-1} over Au/CeO_2[3c] (at 120 °C) and 27 h^{-1} over Ru/Al_2O_3.[6b] The performance in crotyl alcohol oxidation is no less exceptional, with TOF = 7080 h^{-1} achievable at 0.21 atmospheres O_2 and 60 °C, second only to a recently reported AuPd/TiO_2 catalyst that attained 12600 h^{-1}, albeit under 5 atm O_2 and at 160 °C.[5] In contrast, the best literature report for crotyl alcohol selox under comparable reaction conditions, over Ru/Faujisite, achieved a TOF of only 3 h^{-1}.[19] For both alcohols, aldehyde selectivities with our system were better than 91% (Table 1). In absolute terms, redistributing palladium from large metal clusters (4.7 wt%) to Pd^{II} species decorating the mesoporous alumina (0.03 wt%) results in a 30-fold increase in the activity per Pd atom. We also observed an excellent high TOF of 4096 h^{-1} for benzyl alcohol oxidation, which was more than 99% selective for benzaldehyde, thus indicating the applicability of the catalyst beyond allylic systems.

Operando EXAFS measurements confirm that these Pd^{II} centers remain unchanged during the course of reaction over periods of days (unlike other supported Pd systems, for which reduction and sintering occur in situ[7a,9a,11a]) and are therefore unequivocally the active catalytic species. It is important to note that these catalysts are simple to synthesize on a kilogram scale, that they exhibit excellent longevity and recyclability, and that maximum activity is attained concomitant with vast reductions in precious-metal content. Highly dispersed Pd^{II} has been postulated as the active species in Wacker-type partial oxidation in doped $MoVNbO_x$ catalysts.[20]

In conclusion, we have synthesized new mesoporous catalysts that contain atomically dispersed Pd^{II} centers. These materials show exceptional catalytic performance in the aerobic selox of allylic alcohols under mild conditions. The dramatic dependence of cinnamaldehyde production on electron-deficient palladium highlights the parallel between homogeneous and heterogeneous alcohol selox chemistry and the importance of isolated Pd^{II} sites in the catalytic cycle—a discovery that opens new avenues for tailored selox catalysts.

Experimental Section

Alcohol oxidation was performed on a Radleys carousel on a 10-mL scale at 60 °C. Individual reactors were charged with benzyl, cinnamyl, or crotyl alcohol (0.84 mmol, Aldrich, 99%) in toluene (10 mL) with mesitylene as an internal standard. Reactions were performed on air with catalyst (50 mg) and analyzed by GC using a DB5 capillary column. Cinnamaldehyde, crotonaldehyde, and benzaldehyde were the principal reaction products in all cases (87–94% selectivity). There was no evidence for solvent oxidation or alcohol isomerization or polymerization, reflecting our mild operating conditions. Reactions were run for up to 24 h with initial rates determined from the linear portion of the reaction profile. Catalyst selectivity and mass balances (closure was greater than 98%) were determined using reactant and product response factors with quoted conversions and selectivities given to ±2 and ±3%, respectively. All catalyst samples could be recycled by simple filtration, washing with toluene, and air drying without significant loss of activity over three consecutive runs (TOFs remaining within 10% of initial values). Exemplary kinetic profiles are shown in the Supporting Information.

Received: June 11, 2007
Revised: August 30, 2007
Published online: October 5, 2007

Keywords: heterogeneous catalysis · mesoporous materials · oxidation · palladium · X-ray absorption spectroscopy

[1] a) T. Mallat, A. Baiker, *Chem. Rev.* **2004**, *104*, 3037–3058; b) M. Besson, P. Gallezot, *Catal. Today* **2000**, *57*, 127–141.
[2] a) R. A. Sheldon, *Pure Appl. Chem.* **2000**, *72*, 1233–1246; b) R. A. Sheldon, I. W. C. E. Arends, G.-J. ten Brink, A. Dijksman, *Acc. Chem. Res.* **2002**, *35*, 774–781.
[3] a) G. J. Hutchings, S. Carrettin, P. Landon, J. K. Edwards, D. Enache, D. W. Knight, Y.-J. Xu, A. F. Carley, *Top. Catal.* **2006**, *38*, 223–230; b) A. Abad, P. Concepción, A. Corma, H. García, *Angew. Chem.* **2005**, *117*, 4134–4137; *Angew. Chem. Int. Ed.* **2005**, *44*, 4066–4069; c) A. Abad, C. Almela, A. Corma, H. Garcý'a, *Chem. Commun.* **2006**, 3178–3180.
[4] M. D. Hughes, Y.-J. Xu1, P. Jenkins, P. McMorn, P. Landon, D. I. Enache, A. F. Carley, G. A. Attard, G. J. Hutchings, F. King,

E. H. Stitt, P. Johnston, K. Griffin, C. J. Kiely, *Nature* **2005**, *437*, 1132 – 1135.
[5] D. I. Enache, J. K. Edwards, P. Landon, B. Solsona-Espriu, A. F. Carley, A. A. Herzing, M. Watanabe, C. J. Kiely, D. W. Knight, G. J. Hutchings, *Science* **2006**, *311*, 362 – 365.
[6] a) K. Yamaguchi, N. Mizuno, *Angew. Chem.* **2002**, *114*, 4720 – 4724; *Angew. Chem. Int. Ed.* **2002**, *41*, 4538 – 4542; b) K. Yamaguchi, N. Mizuno, *Chem. Eur. J.* **2003**, *9*, 4353 – 4361.
[7] a) K. Mori, K. Yamaguchi, T. Hara, T. Mizugaki, K. Ebitani, K. Kaneda, *J. Am. Chem. Soc.* **2002**, *124*, 11572 – 11573; b) A. F. Lee, J. J. Gee, H. J. Theyers, *Green Chem.* **2000**, *2*, 279 – 282.
[8] a) T. Mallat, Z. Bodnar, A. Baiker, *Stud. Surf. Sci. Catal.* **1993**, *78*, 377 – 384; b) F. Alardin, B. Delmon, P. Ruiz, M. Devillers, *Catal. Today* **2000**, *61*, 255 – 262.
[9] a) J. D. Grunwaldt, M. Caravati, A. Baiker, *J. Phys. Chem. B* **2006**, *110*, 9916 – 9922; b) J. D. Grunwaldt, M. Caravati, A. Baiker, *J. Phys. Chem. B* **2006**, *110*, 25586 – 25589.
[10] A. Corma, *Chem. Rev.* **1997**, *97*, 2373 – 2419.
[11] a) A. F. Lee, K. Wilson, *Green Chem.* **2004**, *6*, 37 – 42; b) A. F. Lee, S. F. J. Hackett, J. S. J. Hargreaves, K. Wilson, *Green Chem.* **2006**, *8*, 549 – 555; c) J. D. Grunwaldt, M. Caravati, M. Ramin, A. Baiker, *Catal. Lett.* **2003**, *90*, 221 – 229.
[12] C. T. Campbell, *Surf. Sci. Rep.* **1997**, *27*, 1 – 111.
[13] F. Vaudry, S. Khodabandeh, M. E. Davis, *Chem. Mater.* **1996**, *8*, 1451 – 1464; see the Supporting Information.
[14] K.-T. Park, D. L. Novikov, V. A. Gubanov, A. J. Freeman, *Phys. Rev. B* **1994**, *49*, 4425 – 4431.
[15] S.-J. Kim, S. Lemaux, G. Demazeau, J.-Y. Kim, J.-H. Choy, *J. Mater. Chem.* **2002**, *12*, 995 – 1000.
[16] S. J. Pennycook, L. A. Boatner, *Nature* **1988**, *336*, 565 – 567.
[17] M. D. Shannon, C. M. Lok, J. L. Casci, *J. Catal.* **2007**, *249*, 41 – 51.
[18] Z. Ma, S. H. Overbury, S. Dai, *J. Mol. Catal. A* **2007**, *273*, 186 – 197.
[19] B.-Z. Zhan, M. A. White, T.-K. Sham, J. A. Pincock, R. J. Doucet, K. V. R. Rao, K. N. Robertson, T. S. Cameron, *J. Am. Chem. Soc.* **2003**, *125*, 2195 – 2199.
[20] D. Linke, D. Wolf, M. Baerns, O. Timpe, R. Schlögl, S. Zeyß, U. Dingerdissen, *J. Catal.* **2002**, *205*, 16 – 31.

